1994

Controlled Biomineralization of Magnetite (Fe₃O₄) and Greigite (Fe₃S₄) in a Magnetotactic Bacterium

Dennis A. Bazylinski

Richard B. Frankel

Brigid R. Heywood

Stephen Mann

John W. King
University of Rhode Island, jwking@uri.edu

See next page for additional authors

Authors

Dennis A. Bazylinski, Richard B. Frankel, Brigid R. Heywood, Stephen Mann, John W. King, Percy L. Donaghay, and Alfred K. Hanson

Controlled Biomineralization of Magnetite (Fe₃O₄) and Greigite (Fe₃S₄) in a Magnetotactic Bacterium

DENNIS A. BAZYLINSKI,[1]* RICHARD B. FRANKEL,[2] BRIGID R. HEYWOOD,[3] STEPHEN MANN,[4]
JOHN W. KING,[5] PERCY L. DONAGHAY,[5] AND ALFRED K. HANSON[5]

*Marine Science Center, Northeastern University, East Point, Nahant, Massachusetts 01908[1]; Department of Physics,
California Polytechnic State University, San Luis Obispo, California 93407[2]; Department of Chemistry
and Applied Chemistry, University of Salford, Salford, M5 4WT,[3] and School of Chemistry,
University of Bath, Bath BA2 7AY,[4] United Kingdom; and Graduate
School of Oceanography, University of Rhode Island,
Narragansett, Rhode Island 02882-1197[5]*

A slowly moving, rod-shaped magnetotactic bacterium was found in relatively large numbers at and below the oxic-anoxic transition zone of a semianaerobic estuarine basin. Unlike all magnetotactic bacteria described to date, cells of this organism produce single-magnetic-domain particles of an iron oxide, magnetite (Fe₃O₄), and an iron sulfide, greigite (Fe₃S₄), within their magnetosomes. The crystals had different morphologies, being arrowhead or tooth shaped for the magnetite particles and roughly rectangular for the greigite particles, and were coorganized within the same chain(s) in the same cell with their long axes along the chain direction. Because the two crystal types have different crystallochemical characteristics, the findings presented here suggest that the formation of the crystal types is controlled by separate biomineralization processes and that the assembly of the magnetosome chain is controlled by a third ultrastructural process. In addition, our results show that in some magnetotactic bacteria, external environmental conditions such as redox and/or oxygen or hydrogen sulfide concentrations may affect the composition of the nonmetal part of the magnetosome mineral phase.

Magnetotactic bacteria are a diverse group of gram-negative procaryotes (6) that orient and navigate along geomagnetic field lines (12). All such bacteria contain magnetosomes (1), which are membrane-bounded (14), intracellular single-magnetic-domain particles of either an iron oxide, magnetite (Fe₃O₄) (2, 13, 21, 24, 30, 35), or an iron sulfide, greigite (Fe₃S₄) (3, 15, 16), or a combination of greigite and iron pyrite (FeS₂) (23). For any given magnetotactic bacterial species or strain, magnetic particles of a specific mineral type, magnetite or greigite, with a specific crystallographic habit are produced (25, 26). Thus, biomineralization of the magnetosome mineral phase is a highly regulated process that is probably directed and controlled at the gene level. In addition, phylogenetic analyses have indicated independent evolutionary origins for magnetotaxis in the iron oxide- and iron sulfide-producing bacteria, suggesting that there is separate control of the bioprecipitation events for these mineral types (10).

In one magnetotactic bacterium that produces greigite and iron pyrite (23), copper appears to be taken up into the magnetosome mineral phase (3). This copper incorporation into the magnetsome appears to be limited to a single magnetotactic species and is apparently dependent on external concentrations of copper in the environment (3). There is currently no indication that the nonmetal part of the magnetosome mineral phase is affected by external environmental parameters.

Recently, in a brief report, we described a unique type of magnetotactic bacterium that was present at the oxic-anoxic transition zone (OATZ) of the southern basin of the Pettaquamscutt River Estuary, Narragansett, R.I., and that pro-duced both magnetite and greigite particles aligned within the same chain in the same cell (5). In this paper, we describe this organism, its ecology, and its magnetosomes, as well as the significance for understanding the biomineralization processes involved in the formation of the magnetic mineral phases and their assembly into chains in magnetotactic bacteria. In addition, this organism may represent the first magnetotactic bacterium in which the nonmetal part of the magnetosome mineral phase is affected by external environmental conditions.

MATERIALS AND METHODS

Sampling site and sample collection. The sampling site was the deepest part (ca. 20 m) of the southern basin of the Pettaquamscutt River Estuary, R.I. This estuary is a semianaerobic basin that is permanently chemically stratified (11, 32, 34). A steep oxygen concentration gradient and the upward diffusion of hydrogen sulfide generated by bacterial sulfate reduction cause the OATZ to occur in the water column, between 3 and 5 m, rather than in the sediments.

Vertical profiles of oxygen concentration and redox potential (E_h) in the water column of the southern basin of the Pettaquamscutt River Estuary were obtained with an electronic sensor array that was lowered from a stable moored platform with a high-resolution winch. The sensors included an oxygen probe and an E_h probe (SeaBird Electronics, Bellvue, Wash.). Water samples were obtained from discrete depths of interest by simultaneously monitoring the vertical profiles with the sensor array and pumping water to the surface with a siphon system that had its intake mounted at the same depth as the sensors. Very low levels of oxygen (<20 μM kg^{-1}) were measured on the water samples by the zinc hydroxide modification of the Winkler method (34). The apparatus and procedures used in chemical profiling and sample collection are described in detail by Donaghay et al. (11).

The vertical distribution of particulate iron and manganese was determined by first filtering 0.5 liter of water through a 0.2-μm-pore-size Millipore tortuous filter, freeze-drying the filter, and then digesting the filter in 50 ml of 2 N HNO₃ in a heated water bath. The final particulate metal concentration per volume of seawater was determined by analyzing the digested sample on a model 3410 inductively coupled argon plasma spectrometer (Applied Research Laboratories, Dearborn, Mich.).

Magnetotactic bacteria were collected from water samples in bottles by the method of Moench and Konetzka (28). Cells were placed on carbon-coated

* Corresponding author. Permanent address: Department of Microbiology, Immunology, and Preventive Medicine, Iowa State University, Ames, IA 50011. Phone: (515) 294-1630. Fax: (515) 294-6019.
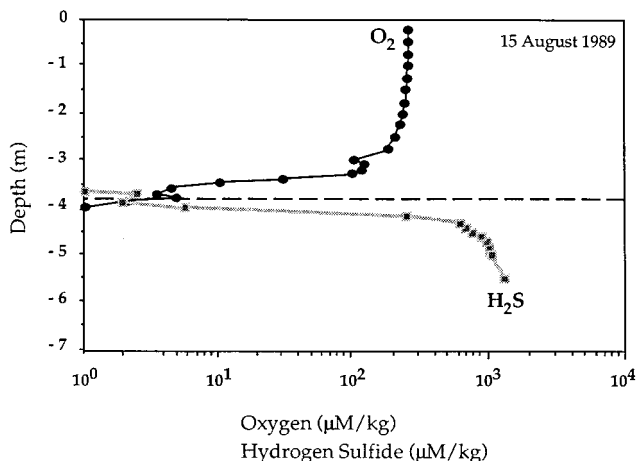
FIG. 1. A typical oxygen and hydrogen sulfide concentration depth profile of the southern basin of the Pettaquamscutt River Estuary. Sampling was performed on 15 August 1989. Modified from reference 32.

nickel electron microscopy grids as previously described (4). The number of cells per depth was determined by first centrifuging a known volume of sample (usually 100 ml) at 10,000 × g for 30 min at 4°C and resuspending the pellet in a much smaller volume of filter-sterilized water (usually 1 ml) from the same depth and then counting the cells directly in a Petroff-Hausser cell-counting chamber. Because less than a numerically significant number of cells were counted even when the samples were concentrated, the numbers reported should be viewed as upper limits.

Electron microscopy and energy-dispersive X-ray analysis. Transmission elec-

tron microscopy examination of whole cells and magnetosomes was performed with various instruments. Simple imaging was carried out with models 200C and 200CX electron microscopes (JEOL, Tokyo, Japan) operating at 200 kV.

Analytical electron microscopy was performed on magnetosomes with a model HB5 VG (Visons Instruments, East Grinstead, United Kingdom) scanning transmission electron microscope (STEM) operating at 100 kV equipped with a field emission gun, a Link LZ-5 X-ray detector, and an AN 10000 X-ray analysis system capable of detecting all elements heavier than boron. Operating parameters of the system and procedures for obtaining elemental X-ray maps of cells and magnetosomes have been previously published (3, 4).

Selected-area electron diffraction. Selected-area electron diffraction measurements on individual magnetosomes were made with a JEOL model 200C electron microscope operating at 200 kV.

RESULTS

Chemical depth profiles of the Pettaquamscutt River Estuary. Previous studies of the vertical structure of the stratified southern basin of the Pettaquamscutt River Estuary indicated the presence of three zones: (i) an oxic zone with abundant molecular oxygen and positive E_h values in the upper 3 to 4 m of the water column; (ii) the OATZ, or microaerobic zone, where oxygen and hydrogen sulfide coexist at low concentrations and E_h values near zero; and (iii) an anoxic zone, where hydrogen sulfide concentrations increase to high levels with a concomitant decrease in E_h to negative values (11, 32). A typical profile is shown in Fig. 1.

Chemical depth profiles from this study are shown in Fig. 2. Oxygen concentrations fell below the detection limit of 20 μM kg of water^{-1} at 3.4 m, whereas the E_h decreased to negative values at 4.6 m. We infer from data obtained by Donaghay et al. (11) that the OATZ was located between about 3.6 and 4.6
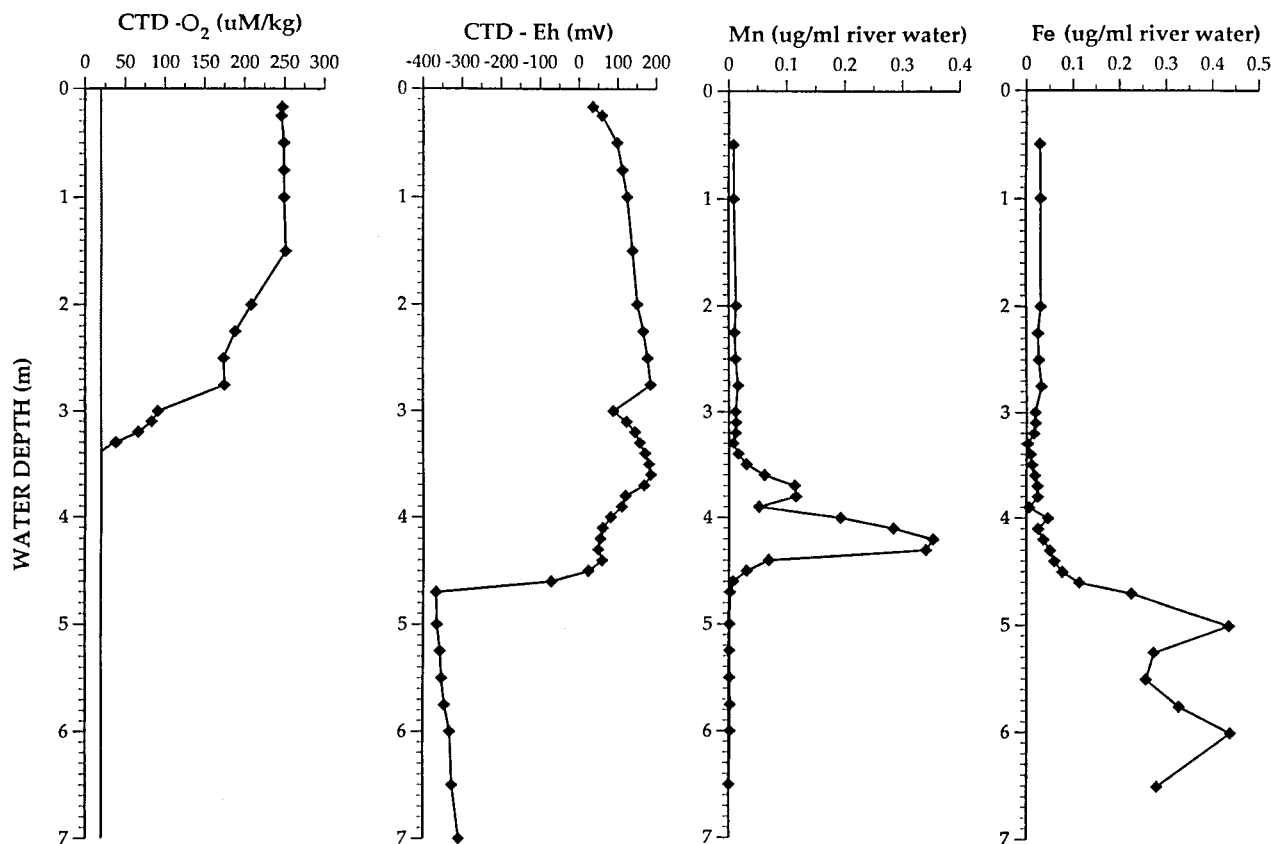

FIG. 2. Depth profiles of CTD-O_2, CTD-E_h, and particulate Mn and Fe concentrations in the southern basin of the Pettaquamscutt River Estuary. Samples were taken on 16 September 1992. The detection limit of 20 μM kg of water^{-1} for the oxygen probe is shown as a vertical line on the oxygen profile.
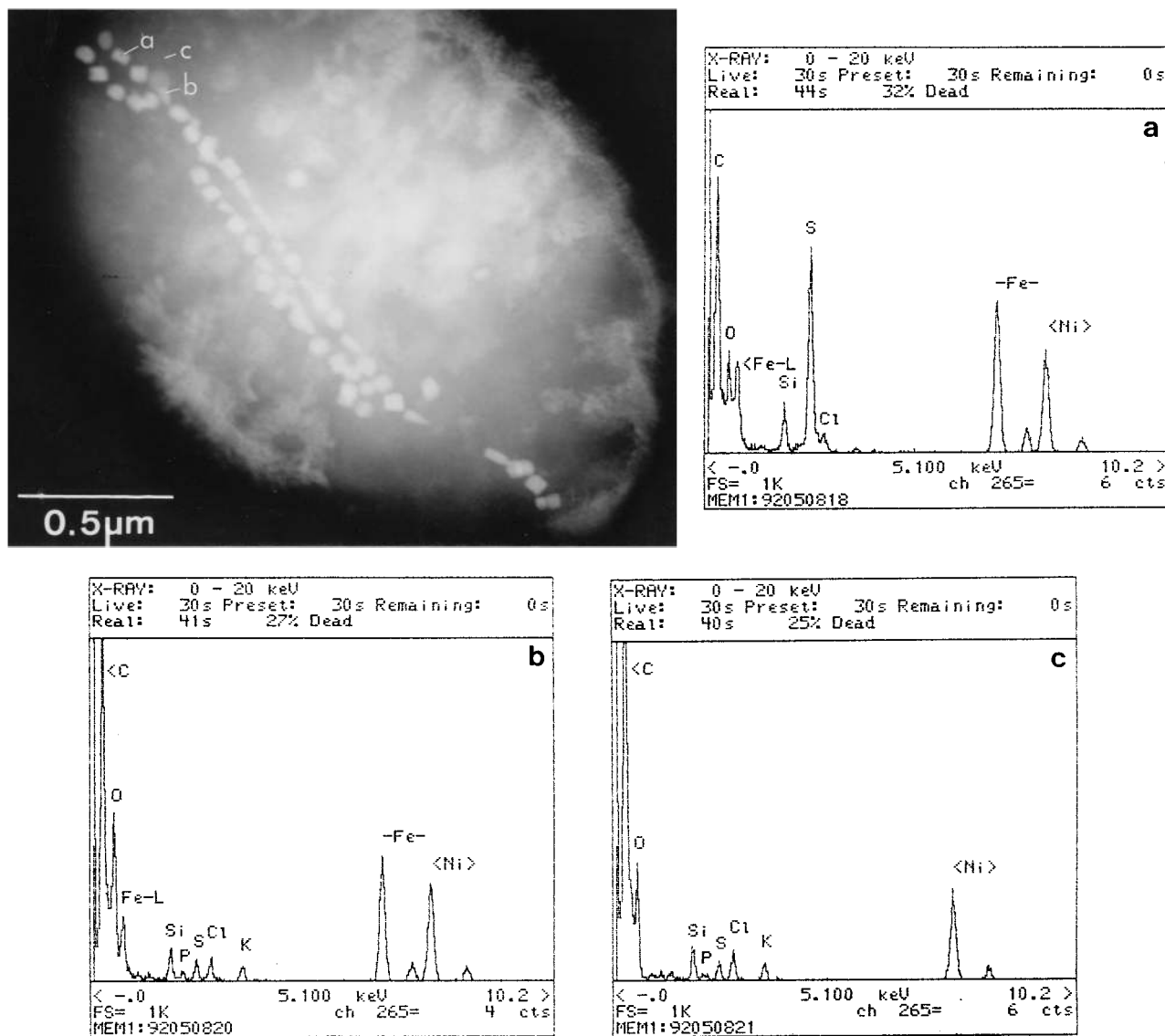
FIG. 3. Dark-field STEM image of a rod-shaped magnetotactic bacterium showing two chains of arrowhead-shaped and roughly rectangular magnetosomes. Letters designate position of electron beam for elemental spectra labeled a to c. (a) Elemental spectra of a rectangular iron-sulfur particle (a in the STEM), an arrowhead-shaped iron-oxygen particle (b in the STEM), and the cellular background (c in the STEM). Note that iron is the only metal in either particle type. The nickel signal is from the electron microscopy grid.

m during our 16 September 1992 field sampling. Anoxic conditions were present below this depth.

Maximum concentrations of particulate manganese (Fig. 2) were found in the OATZ between 3.4 and 4.6 m in association with oxygen concentrations below 20 μM kg of water^{-1}. Concentrations of particulate iron (Fig. 2) started to increase in the lower depths of the OATZ, at about 4.4 m, and reached maximum values in the anoxic zone at about 5 m and below.

Presence of magnetotactic bacteria. Live magnetotactic bacteria were first detected in water samples collected at about 2.25 m and were found down to the lowest sampling depth of 6.5 m. The largest numbers of magnetotactic bacteria occurred between 3.5 and 4.7 m in the OATZ and slightly below. At least seven different morphological types of magnetotactic bacteria were observed, although not at all depths; they included coccoid, helical, vibrioid, and rod-shaped bacteria and even an apparent multicellular form (29). Generally, more magnetite

producers were found in the OATZ and above and more greigite producers were found in the sulfidic, anoxic zone.

The magnetotactic bacterium described below was detected from about 4.2 to 6.5 m. It was the numerically dominant magnetotactic organism at 4.5 m and below. Maximum numbers of live motile cells were found at 4.4 to 4.7 m. We estimate the numbers of these rod-shaped magnetotactic cells present at these depths at the OATZ and slightly below to be between 10^4 and 10^5/ml but regard these values as upper limits. Previous estimates for certain depths were higher at about 2×10^5 cells per ml (34).

Description of the organism. The cells were elliptical to cigar shaped (Fig. 3) and measured, on average, 3.1 by 1.3 μm; they appeared to possess a single polar flagellum. They were slow moving compared with cells of other magnetotactic species but exhibited typical magnetotactic behavior; that is, they aligned parallel to the direction of the magnetic field and
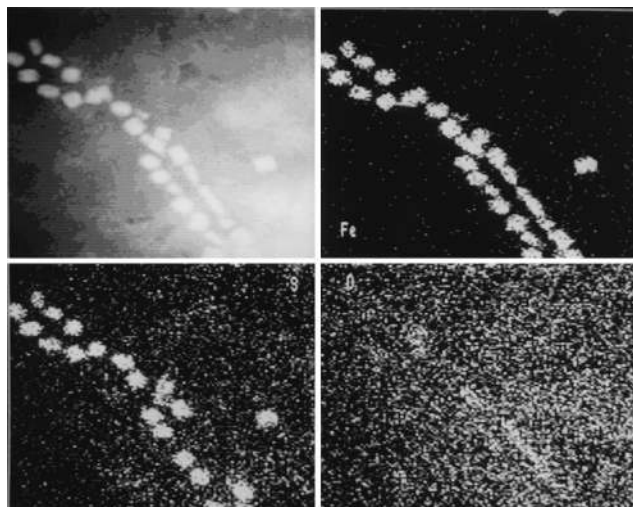
FIG. 4. Dark-field STEM image and iron, sulfur, and oxygen elemental maps, derived from energy-dispersive X-ray analyses of the upper portion of the magnetosome chain within the bacterium shown in Fig. 3. Note that the positions of the arrowhead-shaped particles correlate with the presence of iron and oxygen but not sulfur and that of the rectangular particles correlates with iron and sulfur but not oxygen. The oxygen map has high background because of the abundance of oxygen contained in the organic matter of the cell.

reversed their direction of motility by 180° when the field direction was reversed. More than 99% of the cells collected from water samples were North seeking. When cells were directed to the edge of a water droplet, they rarely showed any backward motion ("two-way" swimming), unlike bipolarly flagellated magnetotactic spirilla (7, 33) or unipolarly flagellated magnetotactic vibrios (2).

Magnetosomes. Cells usually contained two (Fig. 3), but occasionally more, chains of magnetosomes that traversed the cell longitudinally. These multiple chains could be seen within cells under phase-contrast light microscopy as a dark filament which appeared to be anchored to the inner aspect of the cell wall and rotated as the cell rotated while swimming.

Most cells collected from the OATZ and slightly deeper contained two morphologically distinct types of particles in their magnetosomes: elongated arrowhead- or tooth-shaped particles and roughly rectangular particles, both with their long axes oriented along the chain direction (Fig. 3). Both types of particles exhibited strong diffraction contrast, indicating that they were crystalline. Figure 4 shows iron, sulfur, and oxygen elemental maps, derived from energy-dispersive X-ray analyses of both crystal types in part of the chain shown in Fig. 3. Whereas the rectangular particles consisted of iron and sulfur, the arrowhead-shaped particles consisted of iron and oxygen but no sulfur. Elemental energy-dispersive X-ray analysis spectra of individual particles (Fig. 3) further confirmed these results and showed that no other metals were associated with the magnetosomes. Generally, there were approximately three times as many rectangular particles as arrowhead-shaped particles, with relatively more arrowhead-shaped particles in cells collected higher up in the more oxidized regions of the OATZ in the water column (Table 1). When collected from deeper in the anoxic zone, 5.75 to 6.0 m, many cells had rectangular iron-sulfur particles exclusively (Table 1). Because the iron-oxygen crystals did not have an iron-sulfur core (Fig. 4), it is unlikely that the arrowhead-shaped particles represent an oxidation product of the iron-sulfur particles (23).

Single-crystal electron diffraction patterns were obtained

from a number of both types of particles present within a single chain (5). The patterns obtained from the arrowhead-shaped iron-oxygen crystals and the rectangular iron-sulfur crystals were consistent with the face-centered-cubic spinel minerals magnetite and greigite, respectively (5). When cells contained only one type of particle, the diffraction patterns obtained from the arrowhead-shaped particles (Fig. 5a and b) and the rectangular particles (Fig. 5c and d) were also consistent with magnetite and greigite, respectively.

Size dimensions of both magnetite and greigite crystals are shown in Table 1. Particles of each type had similar dimensions regardless of whether they were both present within the same cell or only one type was present in a cell. The arrowhead-shaped magnetite crystals were elongated along the <1 1 1> axis and terminated at one end with a well-defined {1 1 1} face. This crystal morphology is similar to that previously described for magnetite particles in an uncultured freshwater magnetotactic bacterium (21, 22). The rectangular greigite crystals were elongated along the <1 0 0> axis and terminated with two well-defined {1 0 0} faces. This rectangular prismatic morphology is similar to that previously described for greigite particles in other rod-shaped magnetotactic bacteria collected from salt marsh pools (15, 16).

In addition to differences in crystallographic habit, there were differences in the crystallographic orientation of the two particle types along the chain direction. Whereas the long axis of the magnetite particles oriented along the chain was a <1 1 1> crystallographic axis, the long axis of the greigite particles oriented along the chain was a <1 0 0> axis. These respective crystallographic orientations were the same as those previously observed in magnetotactic bacteria with single mineral-type chains (15, 16, 21, 22). Thus, the magnetite and greigite magnetosomes are coorganized in the same chains but retain their respective crystallochemical characteristics in the chain.

DISCUSSION

The OATZ of the Pettaquamscutt River Estuary is a location where a relatively large number of magnetotactic bacteria coexist (34). Most of the morphological types of magnetotactic microorganisms from the Pettaquamscutt River Estuary, including coccoid, rod-shaped, vibrioid, and helical forms, are all similar to other magnetotactic bacteria described to date in that their magnetosome chains have either magnetite or greigite crystals exclusively (never both in the same cell) (4). One apparently unusual exception is a many-celled magnetotactic prokaryote (29) which produces two iron sulfides, greigite and pyrite (FeS_2) (23). However, the magnetotactic rod described here is unique among magnetotactic bacteria in that it contains both a magnetic iron oxide, magnetite, and a magnetic iron sulfide, greigite, in the same cell.

Both the magnetite and the greigite particles are positioned

TABLE 1. Dimensions of magnetite and greigite particles within the cells of a magnetotactic bacterium collected from different depths of the southern basin of the Pettaquamscutt River Estuary

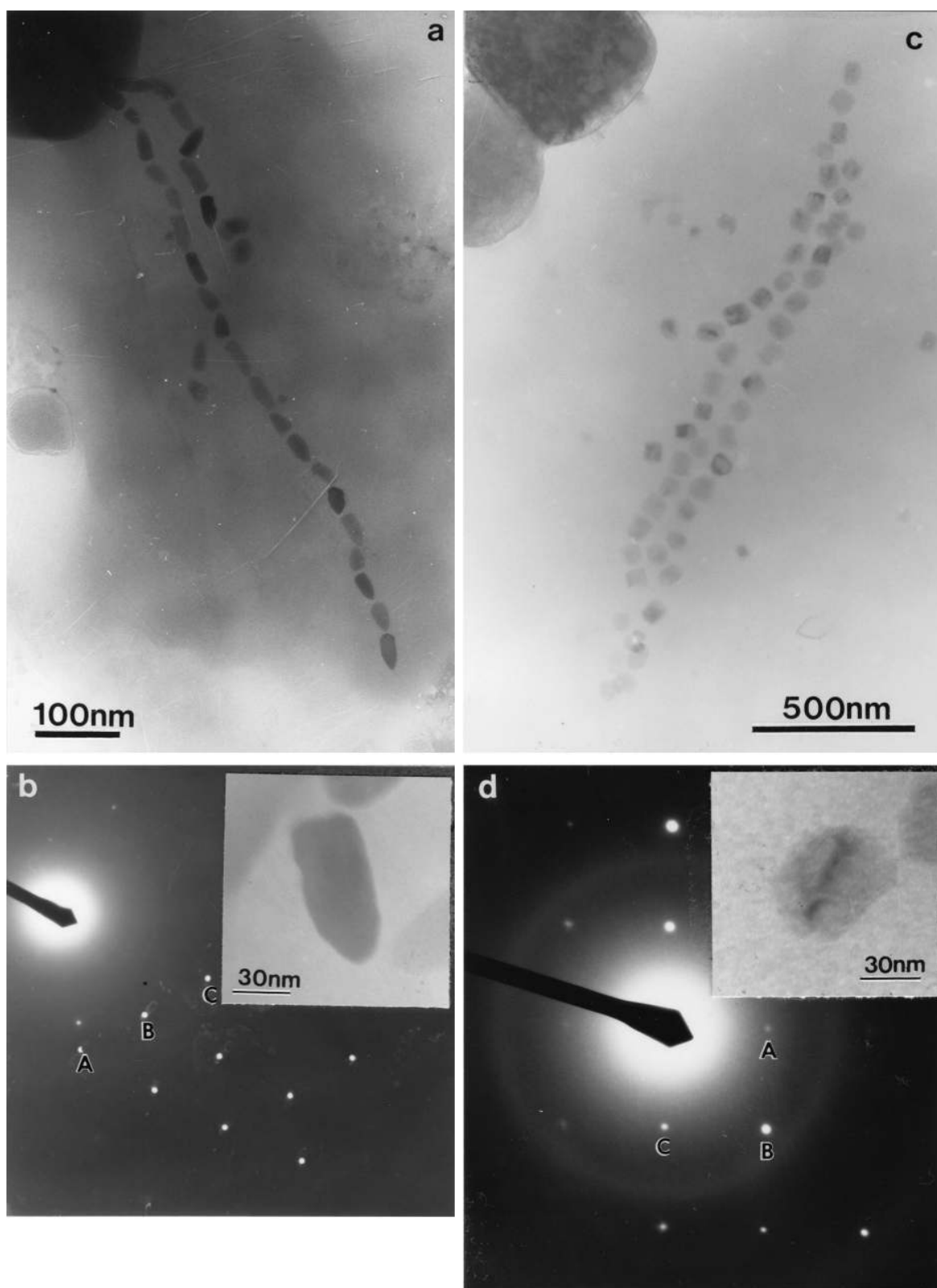| Water depth (m)	Predominant mineral(s) in cells	Total no. of particles per cell[a]	Particle length[a] (nm)	Particle width[a] (nm)
4.6	Fe_3O_4	31 ± 5	63.2 ± 18.3	31.3 ± 8.4
5.5	Fe_3O_4	37 ± 8	64.1 ± 7.7	48.8 ± 6.3
	Fe_3S_4		75.9 ± 1.2	38.4 ± 3.9
5.75	Fe_3S_4	22 ± 4	62.1 ± 13.1	42.7 ± 5.9

[a] Mean ± standard deviation.

FIG. 5. (a) TEM of a chain of magnetosomes in a cell, collected from a depth of 4.6 m, that contained only arrowhead-shaped particles. (b) Single-crystal electron diffraction pattern recorded from an arrowhead-shaped particle in the chain shown in panel a. The inset shows the crystal in the orientation corresponding to the electron diffraction pattern. For the electron diffraction pattern, the camera length and wavelength were 1,025 nm and 0.02508 Å (1 Å = 0.1 nm), respectively. The pattern corresponds to the [1 $\bar{1}$ 0] zone of magnetite, Fe_3O_4. Reflection A (2 $\bar{2}$ 2) (2.43 Å), reflection B (1 1 3) (2.53 Å), and reflection C (0 0 4) (2.15 Å) are also shown. Angles are 2 2 2 × 1 1 3 = 29.5°, 1 1 3 × 0 0 4 = 25.2°, and 2 2 2 × 0 0 4 = 54.7°. Space group Fd3m (cubic); a = 8.396 Å. (c) TEM of a chain of magnetosomes in a cell, collected from a depth of 5.75 m, that contained only roughly rectangular particles. (d) Single-crystal electron diffraction pattern recorded from a rectangular particle in the chain shown in panel c. The inset shows the crystal in the pattern; the camera length and wavelength were 1,025 nm and 0.02508 Å, respectively. The pattern corresponds to the [0 0 1] zone of greigite, Fe_3S_4. Reflection A (2̄ 2 0) (3.49 Å), reflection B (4 0 0) (2.47 Å), and reflection C (2 2̄ 0) (3.49 Å) are also shown. Angles are 2 2 0 × 4 0 0 = 45°, 4 0 0 × 2 2̄ 0 = 45°, and 2 2 0 × 2 2̄ 0 = 90°. Space group Fd3m (cubic); a = 9.876 Å.
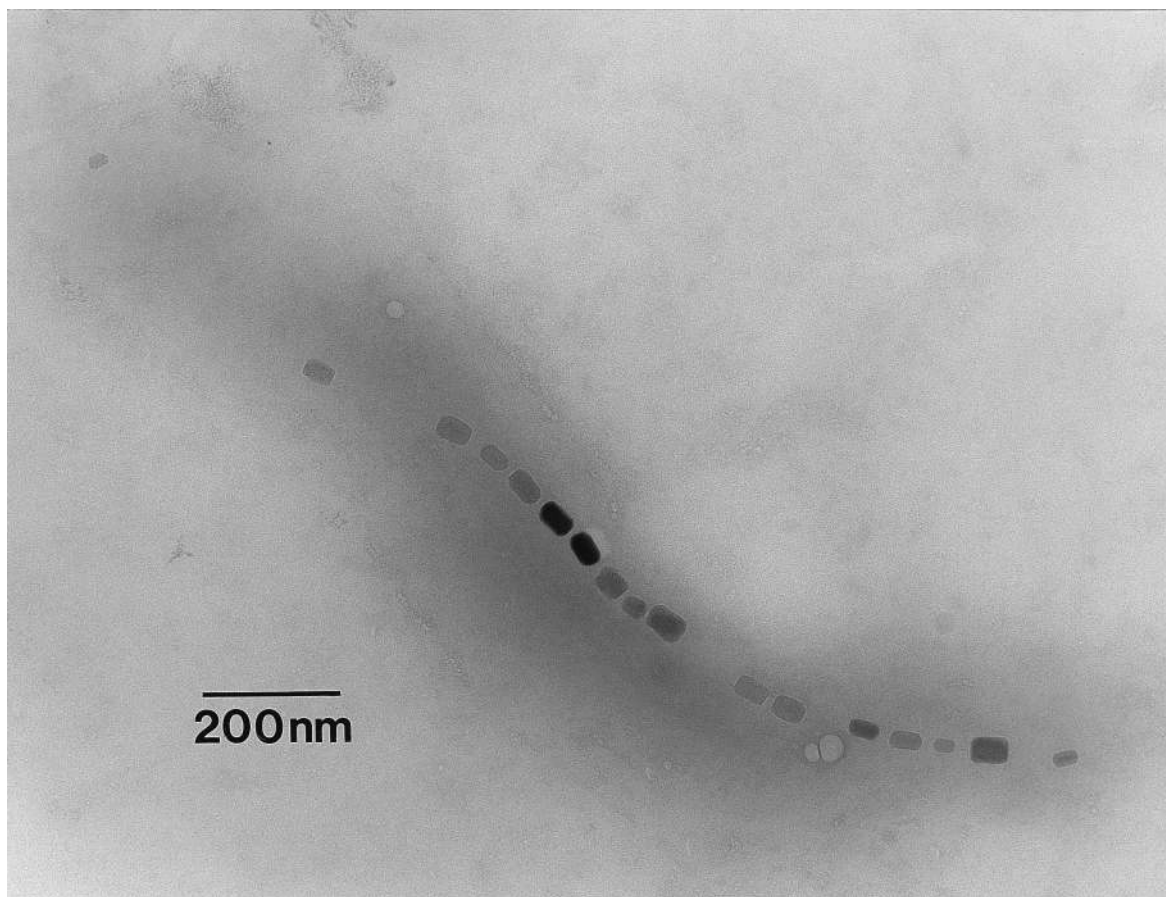
FIG. 6. TEM of an unstained cell of the marine magnetotactic vibrio, strain MV-1. Note that even with the relatively large gaps between some magnetosomes, there is a consistent orientation of each individual magnetosome along the direction of the magnetosome chain, suggesting that the separated magnetosomes are coorganized with the others by a chain assembly process.

within the same chain(s) within the cell, are mineralized with specific sizes and morphologies, and have their long axes oriented along the chain direction. However, the two crystal types have different crystallochemical characteristics, that is, different crystallographic habits and crystallographic orientations with respect to the magnetosome chain. These observations are not consistent with a single biomineralization process in which the crystal type is determined only by environmental conditions, because a single habit and crystal orientation would be expected independent of crystal type. These observations can be rationalized if the cell controls the formation of the two crystal types by independent biomineralization processes and, moreover, controls the assembly of the magnetosome chain by a separate ultrastructural process. Thus, the processes of (i) particle biomineralization and (ii) magnetosome chain assembly are likely to be separately controlled in magnetotactic bacteria. Since the crystallochemical characteristics of the magnetite and the greigite particles in the magnetotactic rod-shaped bacterium described here are similar to those in other magnetotactic bacteria with single-mineral-component chains (15, 16, 21, 22), it is likely that there are independent sets of genes controlling each mineral biomineralization process, again with another gene set controlling magnetosome chain assembly. If this is the case, then the magnetotactic rod-shaped bacterium reported here has both sets of biomineralization genes whereas other magnetotactic bacteria that mineralize only one crystal type have a single set in addition to those regulating magnetosome chain assembly.

A polyphyletic origin for magnetotaxis in bacteria has recently been proposed (10). Phylogenetic analyses showed that a number of magnetite-containing magnetotactic bacteria are associated with the alpha subgroup of the *Proteobacteria* while a greigite-containing magnetotactic bacterium is specifically related to the sulfate-reducing bacteria of the delta subdivision of the *Proteobacteria* (10). The cultured magnetite-containing coccoid and vibrioid magnetotactic bacteria included in this phylogenetic study (strains MC-1, MV-1, and MV-2) did not produce greigite even when grown in culture media containing hydrogen sulfide (25, 26). Furthermore, an anaerobic sulfate-reducing magnetotactic bacterium that produces magnetite while reducing sulfate to sulfide has recently been reported (30). These results are consistent with the existence of independent sets of biomineralization genes for each mineral type. However, the ubiquity of the magnetosome chain motif in magnetite- and greigite-containing magnetotactic bacteria (6, 15, 16, 18, 19) suggests that the ultrastructural elements responsible for magnetosome chain assembly are common to both groups.

Evidence for separately controlled biomineralization and chain assembly processes can also be seen in a freshwater magnetotactic coccus described by Towe and Moench (27, 35), in which the magnetosomes contain magnetite crystals with a

narrow size distribution and a consistent particle morphology (20) but are not organized in chains. This suggests that an intact biomineralization process but a modified or disrupted chain assembly process exists in this organism.

Furthermore, in the marine vibrioid strains MV-1 and MV-2 (2, 26), magnetosomes composed of magnetite with consistent particle morphologies are organized in chains but commonly with relatively large gaps between the magnetosomes in the chain (Fig. 6). However, the separated magnetosomes maintain a consistent orientation with respect to the other magnetosomes. This suggests that the separated magnetosomes are coorganized with the others by a chain assembly process.

The results presented here have important implications for bacterial biomineralization. Magnetotactic bacteria are unusual among prokaryotes in that they have evolved biosynthetic and organizational processes for controlling intracellular biomineralization that appear to be governed by independent parameters. The putative ultrastructural elements responsible for the chain motif would provide a relatively rigid, linear frame for the assembly of magnetosome vesicles prior to mineralization of the mineral phase. In contrast, the nature and development of the associated vesicles themselves are probably species and/or strain specific, since specific mineral compositions and specific crystal morphologies are associated with specific bacterial species or strains (4, 15, 16, 25, 26). The differences in crystallographic orientation and growth characteristics for the magnetite and greigite particles in the magnetotactic bacterium reported here suggest (i) that the magnetosome membranes surrounding the magnetite and greigite crystals contain different nucleation templates and (ii) that there are differences in magnetosome vesicle biosynthesis. In particular, the elongated arrowhead-shaped morphology can be explained by proposing that the surrounding vesicle membrane not only is connected to the structural framework of the chain but also interacts with it dynamically, with scaffolding constituents aligned tangentially to the cell membrane. The greigite crystals, in contrast, are centrosymmetric and not apparently subjected to external stress fields to the same extent.

Generally, the magnetite-producing magnetotactic bacteria were found in the OATZ and above and the greigite producers were found in the sulfidic, anoxic zone. It is noteworthy that cells of the bacterium described here are found in both locations and appear to produce more magnetite when collected from the oxic zone and more greigite when collected from the anoxic, sulfidic zone. This finding suggests that environmental conditions such as local molecular oxygen and/or hydrogen sulfide concentrations somehow regulate the biomineralization process(es) in this organism. Molecular oxygen is known to be required for magnetite synthesis by some magnetotactic species, such as *Magnetospirillum magnetotacticum* (formerly *Aquaspirillum magnetotacticum* [31]) (8), but not others (2, 30). The role of hydrogen sulfide in greigite production by the bacteria that produce it has not been elucidated.

The findings presented here also have important biochemical and paleomagnetic implications. Because magnetotactic bacteria are prodigious accumulators of iron (6), they must certainly play an important role in the cycling of iron, both at the OATZ and in the anoxic zone of stratified marine and estuarine environments. The increase in the particulate iron concentration starting in the lower portion of the OATZ and the maxima at the higher parts of the anoxic zone of the Pettaquamscutt River Estuary are most probably due to the iron oxides and sulfides produced by magnetotactic bacteria. Because the rod-shaped bacterium described here occurs in relatively large numbers at the OATZ and below, it is also likely that this organism is a major contributor to the particu-

late iron concentration as well as to iron cycling in general. Moreover, both the magnetite and greigite particles it contains are within the permanent single-magnetic-domain size range (9, 17). Thus, this is the first instance of a magnetotactic bacterium that can deposit fine-grained particles of both magnetite and greigite that can contribute to the magnetization of sediments.

REFERENCES

1. **Balkwill, D. L., D. Maratea, and R. P. Blakemore.** 1981. Ultrastructure of a magnetotactic spirillum. J. Bacteriol. **141:**1399–1408.
2. **Bazylinski, D. A., R. B. Frankel, and H. W. Jannasch.** 1988. Anaerobic production of magnetite by a marine magnetotactic bacterium. Nature (London) **334:**518–519.
3. **Bazylinski, D. A., A. J. Garratt-Reed, A. Abedi, and R. B. Frankel.** 1993. Copper association with iron sulfide magnetosomes in a magnetotactic bacterium. Arch. Microbiol. **160:**35–42.
4. **Bazylinski, D. A., A. J. Garratt-Reed, and R. B. Frankel.** 1994. Electron microscopic studies of magnetosomes in magnetotactic bacteria. Microsc. Res. Tech. **27:**389–401.
5. **Bazylinski, D. A., B. R. Heywood, S. Mann, and R. B. Frankel.** 1993. Fe_3O_4 and Fe_3S_4 in a bacterium. Nature (London) **366:**218.
6. **Blakemore, R. P., N. A. Blakemore, D. A. Bazylinski, and T. T. Moench.** 1989. Magnetotactic bacteria, p. 1882–1888. *In* J. T. Staley, M. P. Bryant, N. Pfennig, and J. G. Holt (ed.), Bergey's manual of systematic bacteriology, vol. 3. The Williams & Wilkins Co., Baltimore.
7. **Blakemore, R. P., D. Maratea, and R. S. Wolfe.** 1979. Isolation and pure culture of a freshwater magnetic spirillum in chemically defined growth medium. J. Bacteriol. **140:**720–729.
8. **Blakemore, R. P., K. A. Short, D. A. Bazylinski, C. Rosenblatt, and R. B. Frankel.** 1985. Microaerobic conditions are required for magnetite synthesis within *Aquaspirillum magnetotacticum*. Geomicrobiol. J. **4:**53–71.
9. **Butler, R. F., and S. K. Banerjee.** 1975. Theoretical single-domain grain size range in magnetite and titanomagnetite. J. Geophys. Res. **80:**4049–4058.
10. **DeLong, E. F., R. B. Frankel, and D. A. Bazylinski.** 1993. Multiple evolutionary origins of magnetotaxis in bacteria. Science **259:**803–806.
11. **Donaghay, P. L., H. M. Rines, and J. M. Sieburth.** 1992. Simultaneous sampling of fine scale biological, chemical, and physical structure in stratified waters. Arch. Hydrobiol. Beih. Ergebn. Limnol. **36:**97–109.
12. **Frankel, R. B.** 1984. Magnetic guidance of organisms. Annu. Rev. Biophys. Bioeng. **13:**85–103.
13. **Frankel, R. B., R. P. Blakemore, and R. S. Wolfe.** 1979. Magnetite in freshwater magnetotactic bacteria. Science **203:**1355–1356.
14. **Gorby, Y. A., T. J. Beveridge, and R. P. Blakemore.** 1988. Characterization of the bacterial magnetosome membrane. J. Bacteriol. **170:**834–841.
15. **Heywood, B. R., D. A. Bazylinski, A. J. Garratt-Reed, S. Mann, and R. B. Frankel.** 1990. Controlled biosynthesis of greigite (Fe_3S_4) in magnetotactic bacteria. Naturwissenschaften **77:**536–538.
16. **Heywood, B. R., S. Mann, and R. B. Frankel.** 1991. Structure, morphology, and growth of biogenic greigite (Fe_3S_4), p. 93–108. *In* M. Alpert, P. Calvert, R. B. Frankel, P. Rieke, and D. Tirrell (ed.), Materials syntheses based on biological processes. Materials Research Society, Pittsburgh.
17. **Hoffman, V.** 1992. Greigite (Fe_3S_4): magnetic properties and first domain observations. Phys. Earth Planet. Inter. **70:**288–301.
18. **Mann, S., and R. B. Frankel.** 1990. Magnetite biomineralization in unicellular microorganisms, p. 389–426. *In* S. Mann, J. Webb, and R. J. P. Williams (ed.), Biomineralization: chemical and biochemical perspectives. VCH, Weinheim, Germany.
19. **Mann, S., R. B. Frankel, and R. P. Blakemore.** 1984. Structure, morphology, and crystal growth of bacterial magnetite. Nature (London) **310:**405–407.
20. **Mann, S., T. T. Moench, and R. J. P. Williams.** 1984. A high resolution electron microscopic investigation of bacterial magnetite. Implications for crystal growth. Proc. R. Soc. London Ser. B **221:**385–393.
21. **Mann, S., N. H. C. Sparks, and R. P. Blakemore.** 1987. Ultrastructure and characterisation of anisotropic magnetite inclusions in magnetotactic bacteria. Proc. R. Soc. London Ser. B **231:**469–476.
22. **Mann, S., N. H. C. Sparks, and R. P. Blakemore.** 1987. Structure, morphology, and crystal growth of anisotropic magnetite crystals in magnetotactic bacteria. Proc. R. Soc. London Ser. B **231:**477–487.

23. **Mann, S., N. H. C. Sparks, R. B. Frankel, D. A. Bazylinski, and H. W. Jannasch.** 1990. Biomineralisation of ferrimagnetic greigite (Fe_3S_4) and iron pyrite (FeS_2) in a magnetotactic bacterium. Nature (London) **343:**258–260.

24. **Matsuda, T., J. Endo, N. Osakabe, A. Tonomura, and T. Arii.** 1983. Morphology and structure of biogenic magnetite particles. Nature (London) **302:**411–412.

25. **Meldrum, F. C., B. R. Heywood, S. Mann, R. B. Frankel, and D. A. Bazylinski.** 1993. Electron microscopy study of magnetosomes in a cultured coccoid magnetotactic bacterium. Proc. R. Soc. London Ser. B **251:**231–236.

26. **Meldrum, F. C., B. R. Heywood, S. Mann, R. B. Frankel, and D. A. Bazylinski.** 1993. Electron microscopy study of magnetosomes in two cultured vibrioid magnetotactic bacteria. Proc. R. Soc. London Ser. B **251:**237–242.

27. **Moench, T. T.** 1988. *Biliphococcus magnetotacticus* gen. nov. sp. nov., a motile, magnetic coccus. Antonie van Leeuwenhoek J. Microbiol. **54:**483–496.

28. **Moench, T. T., and W. A. Konetzka.** 1978. A novel method for the isolation and study of a magnetotactic bacterium. Arch. Microbiol. **119:**203–212.

29. **Rodgers, F. G., R. P. Blakemore, N. A. Blakemore, R. B. Frankel, D. A. Bazylinski, D. Maratea, and C. Rodgers.** 1990. Intercellular structure in a many-celled magnetotactic procaryote. Arch. Microbiol. **154:**18–22.

30. **Sakaguchi, T., J. G. Burgess, and T. Matsunaga.** 1993. Magnetite formation by a sulphate-reducing bacterium. Nature (London) **365:**47–49.

31. **Schleifer, K.-H., D. Schüler, S. Spring, M. Weizenegger, R. Amann, W. Ludwig, and M. Kohler.** 1991. The genus *Magnetospirillum* gen nov., description of *Magnetospirillum gryphiswaldense* sp. nov. and transfer of *Aquaspirillum magnetotacticum* to *Magnetospirillum magnetotacticum* comb. nov. Syst. Appl. Microbiol. **14:**379–385.

32. **Sieburth, J. M., and P. L. Donaghay.** 1993. Planktonic methane production and oxidation within the algal maximum of the pycnocline: seasonal fine-scale observations in an anoxic estuarine basin. Mar. Ecol. Prog. Ser. **100:**3–15.

33. **Spormann, A. M., and R. S. Wolfe.** 1984. Chemotactic, magnetotactic and tactile behaviour in a magnetic spirillum. FEMS Microbiol. Lett. **22:**171–177.

34. **Stolz, J. F.** 1992. Magnetotactic bacteria: biomineralization, ecology, sediment magnetism, environmental indicator, p. 133–145. *In* H. W. C. Skinner and R. W. Fitzpatrick (ed.), Biomineralization processes of iron and manganese: modern and ancient environments. Catena, Cremlingen-Destedt, Germany.

35. **Towe, K. M., and T. T. Moench.** 1981. Electron-optical characterization of bacterial magnetite. Earth Planet. Sci. Lett. **52:**213–220.